# IMPROVED SURFACE WAVE DISPERSION MODELS AND AMPLITUDE MEASUREMENTS

Jeffry L. Stevens, David A. Adams, and Mariana G. Eneva

Science Applications International Corporation

Sponsored by Air Force Research Laboratory

Contract No. DTRA01-01-C-0082

## ABSTRACT

Surface waves are of primary importance for nuclear monitoring because the $M_s$:$m_b$ discriminant and its regional variants are among the most reliable means of determining whether an event is an earthquake or an explosion. The primary goal of this project is to reduce the magnitude threshold for which surface waves can be identified and measured reliably and to improve the accuracy of surface wave measurement using phase-matched filtering and global regionalized earth and dispersion models.

Global regionalized earth and dispersion models are being developed by inversion of a very large data set of phase and group velocity dispersion measurements. The complete data set now contains over one million dispersion data points. The dispersion measurements are inverted for earth structure, and the earth structure is then used to generate dispersion predictions. This is accomplished in the following way. The inversion is performed for approximately 600 distinct base structures, which were originally derived from the Crust 2.0 models over the AK135 mantle model. The Moho depth, bathymetry, and sediment depths vary on a one-degree grid. Moho depths are derived from Crust 2.0, sediment depths from the Laske and Masters sediment maps, and bathymetry from ETOPO5. Moho depth, bathymetry, and sediment properties are fixed in the inversion, while crust and upper mantle velocities are allowed to vary in the base models. Phase and group velocity dispersion curves are calculated for each of 64,800 models on the one-degree grid. The phase velocity dispersion curves are then used to calculate phase-matched filters to improve detection.

One of the difficulties of performing such a large, heterogeneous inversion is finding optimum values for smoothing and damping (regularizing) parameters. This is important because too much smoothing/damping will increase data misfit, and too little will produce unrealistic earth models. In this case, smoothing minimizes the gradient of each structure between specified discontinuities, while damping minimizes the difference between the model and the starting model. Discontinuities occur at the Moho and at the base of the surface sediments. In a few cases where there is sufficient high frequency information to resolve shallower structure, inversion is performed for deeper sediments, which introduces another discontinuity. A significant improvement in the inversion procedure over the past year has been the introduction of the capability to vary damping and smoothing parameters for each model. This allows us to improve the data fit for many models, while still retaining realistic earth models in all areas. We are performing 2D inversions (inversion of dispersion at discrete frequencies to form spatial dispersion maps) to identify regions where additional parameterization is needed in the 3D inversions. The additional parameterization takes the form of introduction of new base structures, merging of base structures, or adjustments to boundaries between base structures.

In addition to improving earth and dispersion models, we have implemented and tested procedures for measuring surface wave amplitudes at short periods (5-15 seconds) and at regional distances. We are identifying optimum procedures for measuring path corrected spectral magnitudes and then comparing the results with other procedures, such as Marshall-Basham amplitude corrections, which were designed to correct time domain amplitudes for frequency and structure dependence. Path corrected spectral magnitudes should be independent of distance and only weakly dependent on frequency for shallow events. At higher frequencies and longer distances the amplitude correction depends on having accurate Q models. We find that the best procedure is to measure surface wave amplitudes at periods greater than 14 seconds at all distance ranges for three reasons: 1) earthquake spectra tend to decrease with frequency, degrading discrimination; 2) unlike time domain measurements, spectral measurements can be made accurately at lower frequencies at close distances; and 3) S/N remains higher at periods greater than 14 seconds even for very close distances.

## OBJECTIVE

The goal of this project is to reduce the magnitude threshold for which surface waves can be identified and measured reliably, and to improve the accuracy of surface wave measurement, using phase-matched filtering, development of global regionalized earth and dispersion models, and other techniques.

## RESEARCH ACCOMPLISHED

During the second year of this project, we have focused on two topics: improvements to global earth models and dispersion maps, and improved techniques for measuring surface wave amplitudes. During the first year we completed work on implementation and testing of azimuth estimation techniques at three component stations based on polarization analysis (Stevens et al, 2002).

### Global Earth Models and Surface Wave Dispersion Maps

To improve the detection (e.g. by phase matched filtering) and measurement of surface waves it is important to make good predictions of their dispersion. In our work, surface wave dispersion predictions are based on dispersion measurements for ray paths from all over the globe. We make these predictions via models of the earth. Alternate methods could be developed which would depend on interpolation schemes, such as kriging and which would not make use of earth models. An important advantage gained from using earth models is that we can include information from other studies leading to physically reasonable constraints on dispersion. For our earth models this information consists of the boundaries between geologic zones, bathymetry of oceans, thicknesses of sediments and ice, Moho depths, and prior estimates of seismic velocities derived from Crust 2.0 and AK 135 earth models. These constraints are especially important for filling in the gaps found in the path coverage of our data set and they enable prediction along paths unlike any of the paths in the data set. We perform by non-linear least squares inversion of the dispersion data for two types of models. First are 3D earth models where the adjustable parameters are the shear wave velocities of layers. Second are 2D group velocity models determined by inverting dispersion measurements made in narrow frequency bands. The 2D models are used as a guide in the parameterization of the 3D earth model.

### Description of 3D earth model

The 3D earth model is described briefly here and in greater detail in Stevens et al. (2002). It consists of 1ºx1º blocks and is made up of layers of ice, water, sediments, crust and upper mantle. Currently this model depends on 8918 free parameters, which are adjusted by least squares fitting to Rayleigh wave dispersion data. The free parameters are the S-wave velocities of layers of 572 different model types. Other constrained parameters in the model are P wave velocities, densities and Q. The model types are based on the Crust 2.0 2ºx2º crustal types (Bassin et al., 2000 and Laske et al. 2001) and also on ocean ages (Stevens and Adams, 2000). The top few km of the model (consisting of water, ice and/or sediments) are fixed and match data from one degree bathymetry maps made by averaging Etopo5 five minute measurements of topography, and Laske and Masters (1997) 1 degree maps of sediments. There is an explicit discontinuity between the bottom of the sediments and the crust. There are three or more crustal layers. The Crust 2.0 models, which were the starting point for these structures have three crustal layers, but we found it necessary to add more layers in regions of thick crust. There is another explicit discontinuity at the Crust/Mantle boundary. The Moho depth is derived from Crust 2.0 and varies on a 2º grid. The mantle starting model is derived from AK135 (Kennett, et al, 1995). With these constraints, the inversion is performed for the shear velocity of the crust and upper mantle to a depth of 300 km. Below 300 km the earth structure is fixed, and the inversion model is required to be continuous with the mantle structure at the base of the inversion. In broad ocean areas, we replace the Crust 2.0 model with models distinct for each ocean and subdivided by ocean age. We also separate into distinct models Crust 2.0 models that are geographically separated. So, for example, if Crust 2.0 has the same model type in North America and in Asia, we use the same starting model for each, but treat them as separate models in the inversion.

### Surface wave dispersion data set

During the second year of our project we added three new sets of dispersion data and improved one already existing set bringing the total number of Rayleigh wave dispersion measurements with frequencies greater than or equal to .01 Hz to more than 1,000,000. One new set comes from Los Alamos National Laboratory (Yang et al, 2002) consisting of more than 37,000 dispersion measurements (2009 individual paths) from Central Asia ranging between 0.05 Hz and 0.23 Hz. One other set, not yet reviewed by us, comes from Huang et al (2003) and consists of more than 285,000 data points (9730 paths) from China and another consists of nearly 14,000 our own measurements

from Eurasia. Pre-existing data coming from University of Colorado (Levshin et al, 2002) was improved by relocating events to the hypocenters in Engdahl et al (1998) where possible. Other data already in the data set are described in Stevens et al (2001a,b and 2002). Figure 1 shows the frequency distribution of group velocity measurements in our data set. Phase velocity measurements are dominated by a set coming from the global phase velocity model of Ekstrom et al. (1996), and there are fewer phase velocity measurements at high frequencies.

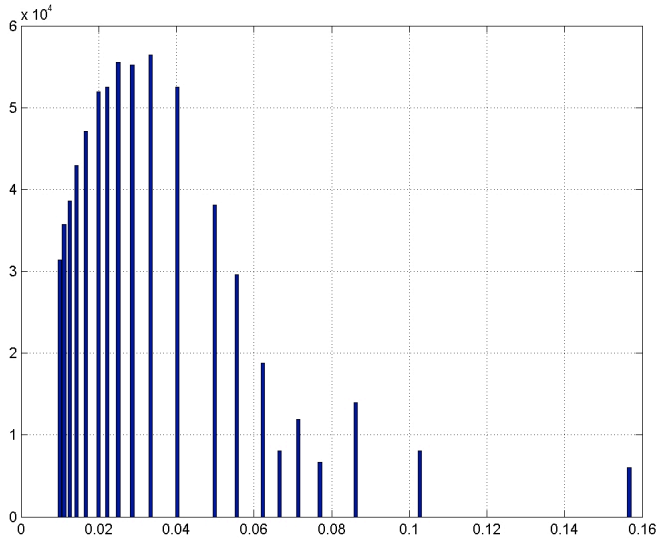


**Figure 1. Bar graph of the number of group velocity measurements in each frequency band for all data currently used in the tomographic inversions**

**The inversion procedure for the 3D earth model**

The relationship between dispersion and the shear wave velocities of the layers in the earth model is non-linear, so the shear wave velocities are estimated by non-linear least squares. At each step a system of tomographic equations is formed, augmented by additional equations of constraint and then solved by the LSQR algorithm. The equations solved are

$$\begin{bmatrix} A \\ sH \\ \beta I \end{bmatrix} \vec{x} = \begin{bmatrix} \vec{l} \\ sH\vec{x}_0 \\ \beta \vec{x}_0 \end{bmatrix} + \begin{bmatrix} \vec{\varepsilon} \\ \vec{\eta} \\ \vec{\zeta} \end{bmatrix},$$

where **x** is the vector of slowness adjustments to the shear wave slownesses of layers in each of the 572 model types. **l** is the vector of slowness differences between predicted and observed dispersion measurements. $\varepsilon$ is the vector of residuals that remain after inversion (the inversion minimizes $|\varepsilon|$). $\mathbf{x_o}$ is the vector of slownesses estimated in the last iteration. The elements of the matrix **A** consist of partial derivatives of dispersion predictions with respect to shear wave slownesses in each layer. **H** is a difference operator that applies to vertically neighboring layers and has the effect of constraining the vertical smoothness of velocity profile. **s** is the weighting of the importance of the smoothness constraint and can be a diagonal matrix (for variably weighted smoothing) or a scalar (constant smoothing). We have implemented variable smoothing so that a different smoothing parameter can be selected for each model type. Lateral smoothing, which is usually applied in tomography studies, is executed indirectly in our study through selection of the model types. **I** is the identity matrix and $\beta$ weights the damping that constrains the norm of the difference between final slownesses and constraining model slownesses (in our work usually the Crust 2.0 values). $\beta$ can be a scalar for constant damping, or a diagonal matrix for variable damping. As for smoothing, variable damping is implemented so that a different parameter can be selected for each model type.

**Regularization and predictions**

Choosing regularizing parameters is an essential part of finding a model which best predicts dispersion, since regularization acts both to control the influence of data noise on the estimation of model parameters and to constrain parts of the model that are poorly constrained by data. Too much regularization will make the model too smooth and too little regularization will allow noise to be projected into the model, making it rough. In this study the damping and smoothing constraints and their associated weighting parameters are used to regularize the solution. Techniques for optimization of regularization parameters are not yet mature, especially for large-scale problems such as this. The methods most often described (e.g. Hansen, 1998) are the L-curve, generalized cross validation, and discrepancy principle. In the literature the first two methods are usually applied to smaller scale problems than ours and with only one regularizing parameter, whereas we have at least 2 and possibly many more. The last method mentioned requires a reliable independent estimate of data noise and works by selecting the regularization resulting in the residual based estimate of noise being the same as the independent one. We have experimented with several of these techniques for our inversion problem, but have not found any reliable enough to replace analyst review of the inversion results.

**Techniques for evolving earth models**

The selection of model types and regularizing parameters are interrelated. For example making a parameterization finer (i.e. adding new model types) without increasing data coverage increases the need for regularization. Our approach for finding a best predictive model has been to start with a small number of model types and increase this number gradually as new data become available or when we detect systematic data misfit. Once a new parameterization is determined, the regularizing parameters are adjusted.

To determine whether there are enough model types, we carry out 2D inversions of group velocity residuals in at least 12 narrow frequency bands to determine group velocity adjustment maps at 1-degree resolution. Each 2D inversion of group velocity residuals is regularized with a damping parameter, which constrains the norm of the group velocity adjustment, and a smoothing parameter which weights a first difference operator that constrains lateral smoothness of the estimated group velocity (i.e. v+$\delta$v). We vary these two parameters for each frequency band to find the smoothest looking map that still reduces data misfit reasonably. The resulting maps are examined to find areas of similar adjustment common to most frequency bands, which are then used to delineate new model types.

After the model types are selected the damping and smoothing parameters (scalars, or diagonal matrices) $\delta$ and **s** are adjusted to find a reasonable looking model that still fits the data adequately. Currently we are experimenting with spatially variable regularization using diagonal matrices rather than scalars. We find that the sensitivity of slowness adjustments to scalar regularization parameter settings is not uniform and depends on model type. In other words when comparing adjustments for different combinations of scalar pairs (s, $\delta$), there is much less variation for some model types than others (see for example Figure 2). The strategy we are now developing is to relax regularization for those types that are relatively insensitive to regularization, and to increase it for those model types that are too sensitive to it.

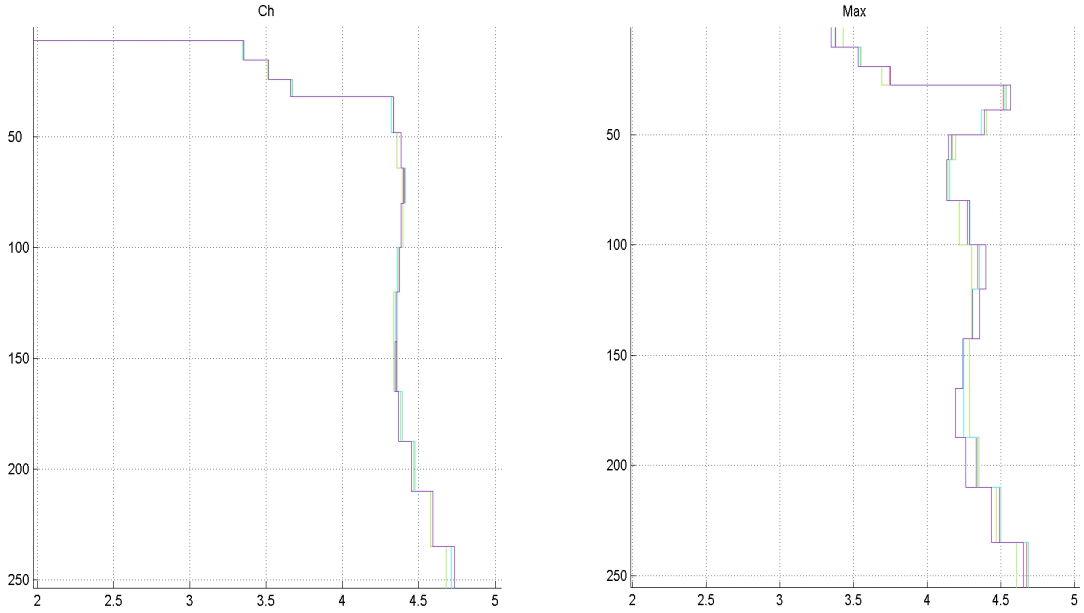


**Figure 2. Shear velocity profiles for two model types: less sensitive to regularization on the left and more sensitive on the right. Ch is from the Yellow Sea and Max is from North East of Mexico. The different structures correspond to different combinations of the scalar regularization parameters s and $\delta$.**

**Data statistics for best current 3D earth model**

The means and standard deviations of normalized group velocity residuals, $1-v_o/v_p$, where $v_o$ and $v_p$ are observed and model predicted group velocities, were calculated for narrow frequency bands and are shown in Figure 3. Solid is

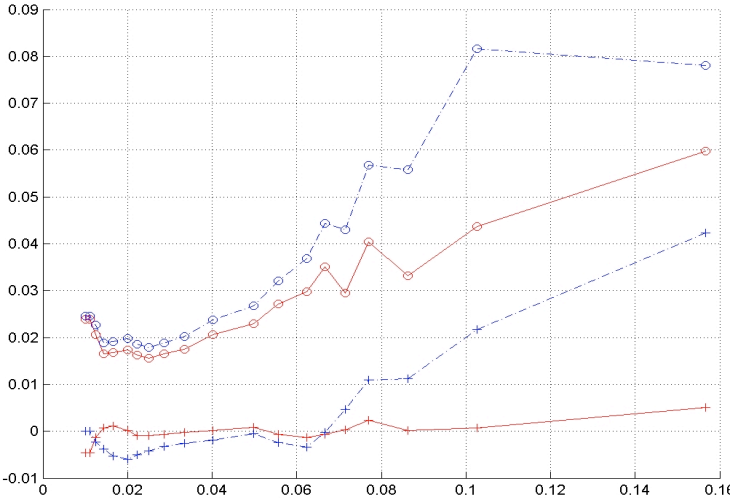


**Figure 3. Standard deviations (o) and means (+) of normalized group velocity residuals are plotted against frequency for 1degree earth model (solid red) and 5-degree earth model (dashed blue).**

for our best 1-degree model, and dashed is for the best 5-degree model (e.g. Stevens and Adams, 2000) based on Crust 5.1 (Mooney, et al., 1998). Figure 3 shows the value of the 1-degree model, especially for high frequencies.

**Optimization of Surface Wave Amplitude Measurements**

Surface wave measurements traditionally are accomplished by measuring a time domain amplitude at a period near 20 seconds. This procedure is problematic at regional distances because the surface wave is not well dispersed and a distinct 20-second arrival may not be present. It is possible to measure time domain amplitudes at higher frequencies with corrections (e.g. Marshall and Basham, 1972), however measurements may be inaccurate due to differences in dispersion caused by differences in earth structure. Stevens and McLaughlin (2001) suggested as an alternative replacing time domain measurements with a path corrected spectral magnitude. The path corrected spectral magnitude is calculated by dividing the observed surface wave spectrum by the Green's function for an explosion of unit moment. The path corrected spectral magnitude is the logarithm of this ratio, and can be estimated over any desired frequency band. This path corrected spectral magnitude is denoted by $\log M_0$.

The advantages of using $\log M_0$ instead of the traditional surface wave magnitude $M_s$ are that $\log M_0$ is insensitive to dispersion, independent of distance, works well at regional distances, and is inherently regionalizeable. Regionalized path corrected spectral magnitudes incorporate geographic variations in source excitation and attenuation. Furthermore, as discussed below, it can in principle be measured over different frequency bands to optimize the signal-to-noise ratio. $M_s$ and $\log M_0$ share some limitations: spectra from earthquakes vary due to source mechanism and depth, and errors can occur if the measurement is made in a spectral dip or at high frequencies for a deep event. Azimuthal variations in amplitude caused by focal mechanism also affect the amplitudes of both $\log M_0$ and $M_s$.

The test cases discussed by Stevens and McLaughlin (2001) used a frequency band of 0.02-0.05 Hz (50-20 s) to estimate the spectral magnitudes. They estimated that on average, the time domain and spectral magnitudes are related as $\log M_0 = M_s + 11.25$. Most of the waveforms in that work were recorded at distances exceeding $8^0$. Due to the relatively flat spectra over the 0.02-0.05 Hz band for most data, this choice worked quite well. The authors noted, however, that higher frequencies might be required for shorter paths. An important observation was that the $\log M_0$ residuals are independent of distance, despite the simple $Q$ models used in the earth structures.

In the present work we focus on the utility of higher frequencies in estimating spectral magnitudes of smaller events, recorded at smaller distances. The purpose is to optimize the spectral magnitude estimates, to test their distance and frequency independence, and to identify any measurement problems or pitfalls. For large amplitude signals we can expect the lower frequencies to be better in general, particularly at larger distances due to greater attenuation at higher frequencies. Our hypothesis at the initiation of this study was that using higher frequencies for measuring spectral magnitudes at shorter distances would optimize signal to noise ratio and therefore be better for measuring surface waves at regional distances, however as discussed below this is only true to a limited extent.

To optimize the measurement procedures and examine the performance of the path corrected spectral magnitude at regional distances, we use 584 spectra from 76 earthquakes and 11 explosions in the Lop Nor area (Figure 4). Additional spectra are available from these events, but only the above spectra were deemed to be of good quality. This means that they passed the dispersion test described by Stevens and McLaughlin (2001) and were checked for certain anomalies such as incorrect instrument calibrations. Approximately 11% of the spectra used for the $\log M_0$ estimates originate from records at source-station distances of $5^0$ or less, and another 11% at distances of $30^0$ or greater. Thus the bulk of the data comes from intermediate distances. Figure 5 shows examples of explosion and earthquake

path corrected spectra from Lop Nor at various distances. The tendency of the explosion spectra to be relatively flat over more extended frequency bands compared with earthquake spectra is evident. This is expected because 1) the spectra are corrected by an explosion Green's function that flattens earthquake spectra imperfectly, and 2) the earthquake spectra have frequency variations caused by source mechanism and depth.

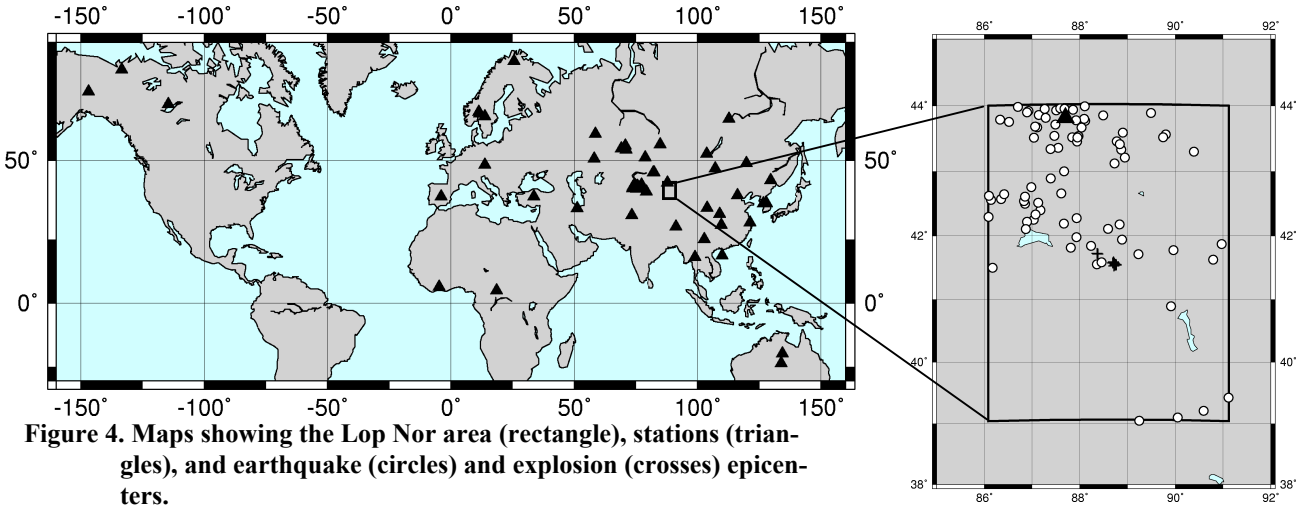


**Figure 4. Maps showing the Lop Nor area (rectangle), stations (triangles), and earthquake (circles) and explosion (crosses) epicenters.**

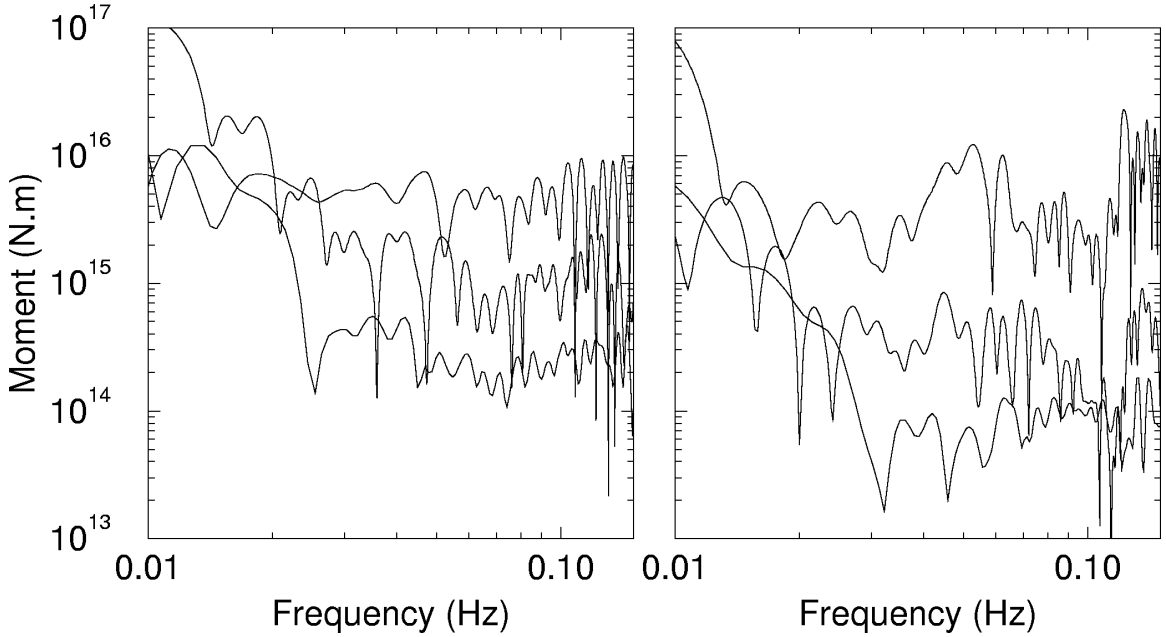


**Figure 5. Examples of path corrected spectra used in this work: (a) Lop Nor explosions recorded at distances of 2°, 7° and 67° (left); (b) Lop Nor earthquakes recorded at distances of 0.4°, 22° and 65° (right). See examples of station log$M_0$ estimates in Table 1. S/N is good at all but the highest frequencies. Instrument responses are uncertain below 0.02 Hz.**

We calculated individual spectral magnitudes (i.e., several station magnitudes per event) over all possible frequency bands between 0.02 Hz (50 s) and 0.15 Hz (~7s), with bandwidths of 0.03 Hz, 0.04 Hz, etc., up to 0.13 Hz for the 0.02-0.15 Hz band. This procedure provided 153 bands to examine from each spectrum. In the search for the most robust spectral magnitude estimate, four different methods were used as follows.

1. Calculating a "simple" mean of the logarithms of all path corrected amplitude measurements made in a given frequency band. This is comparable to Stevens and McLaughlin's (2001) estimates in the 0.02-0.05 Hz band.

2. Iteratively calculating a "robust" mean, by rejecting outliers outside two standard deviations from the mean calculated at each step. The procedure ends when all measurements remain within two standard deviations or when half of the amplitude measurements in a frequency band are rejected, whichever occurs first. Thus the spectral magnitude estimates are much less affected adversely by the tendency of some spectra to sharply vary in amplitude over some frequencies, with most outliers marking anomalously low amplitudes (see Figure 5 above). Figure 6 compares the individual (station) log$M_0$ estimates from (1) and (2). Standard deviations from the robust-mean method are predictably lower than those in the simple-mean method, as the insets in Figure 6 show.
3. Calculating log$M_0$ at the center frequency of a least-squares straight line fit to the spectrum over a given frequency band.
4. Same as (3), but the straight line is "robust", minimizing the absolute deviations of the logarithms of the amplitudes from the line.

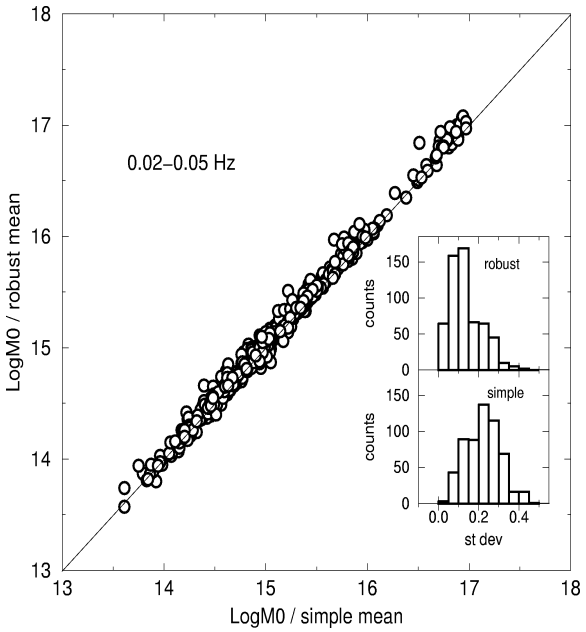


**Figure 6. Comparison of station spectral magnitudes calculated with two different methods. Insets show standard deviations as indicated. See text for details.**

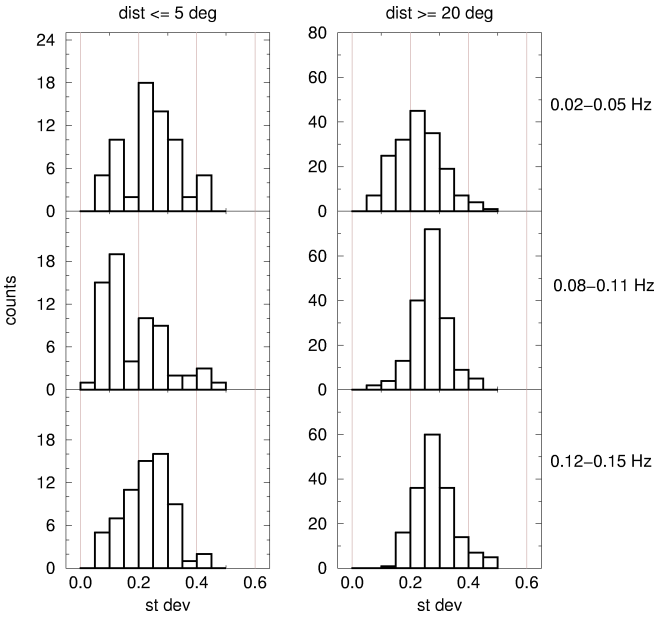


**Figure 7. Histograms of standard deviations of the mean station log$M_0$ estimated in three frequency bands (shown on right), for small and larger distances (shown on top).**

The above estimates were compared in order to select the most suitable frequency bands, possibly varying with distance. Ideally, the corrected spectra would be flat over an extended band of frequencies. Flatness is particularly expected for explosions, as supported (within limits) by the explosion examples in Figure 5 above. The magnitude spectra estimated over any reasonable band would be then consistent. In reality, truly flat spectra over extended frequency bands are rare, so we need to choose bands small enough not to include too many variable features of the spectra, yet large enough not to reflect only local, possibly spurious, characteristics.

In view of the above, the two main desirable properties of a spectrum over a given frequency band are small standard deviations and flatness. For this reason, in our search for optimum frequency bands we used two criteria. First, small standard deviations from (1) above represent one measure of the suitability of a frequency band. Figure 7 indicates that for small distances, the 0.08-0.11 Hz frequency band may be preferable (the largest number of small standard deviations) to either 0.02-0.05 Hz, or 0.12-0.15 Hz. Larger distances do not present a clear picture, but it is still evident that relatively more small standard deviations are found in the 0.02-0.05 Hz frequency band, compared with the higher frequencies. We note that at this stage we do not use the standard deviations from (2), since they are designed to greatly diminish the presence of outliers and are thus not representative enough of the quality of the estimates in the different frequency bands. However, once a suitable frequency band is chosen, the robust mean is the

most reliable estimate of log$M_0$. Spectral flatness as measured with the slopes of the "robust" lines in (4) above provides a second measure of the quality of frequency band; the smaller the slope, the flatter the spectra. Table 1 shows examples of selected estimates, over one specific frequency band out of 153 (0.05-0.1 Hz), for the explosion and earthquake spectra shown in Figure 5. Smaller slopes (flatter spectra) are evident for explosions compared with earthquakes. On the other hand, increasing absolute values of slopes and standard deviations are seen for earthquakes with increasing distance. This is to be expected, as the relatively high-frequency band in the example is less suitable as distance increases.

**Table 1. Station Log$M_0$ estimates in 0.05-0.10 Hz from the spectra in Figure 5**

| *Event Type* | *ID.station* | *Distance, degrees* | *Station log$M_0$ (simple)* | *Station log$M_0$ (robust)* | *Station slope/log$M_0$* | $m_b$ |
|---|---|---|---|---|---|---|
| Explosions | 21450528.WMQ | 2.2 | 14.31+0.10 | 14.33+0.08 | +1.02/14.31 | 4.5 |
| | 21450535.MAK | 7.1 | 15.60+0.15 | 15.67+0.05 | +0.41/15.64 | 5.8 |
| | 21450534.ESDC | 66.8 | 14.95+0.22 | 15.02+0.09 | +1.62/14.97 | 5.4 |
| | | | | | | |
| Earthquakes | 21456615.WMQ | 0.4 | 13.92+0.14 | 14.01+0.05 | +3.64/13.93 | 3.2 |
| | 21456712.ARU | 22.2 | 14.44+0.25 | 14.44+0.24 | -8.70/14.48 | 3.8 |
| | 21457058.ILAR | 65.3 | 15.55+0.27 | 15.45+0.10 | -11.18/15.59 | 4.3 |

Next, we examined the consistency of spectral magnitude estimates in different frequency bands. Figure 8 shows examples of such estimates in several frequency bands (marked along the plot axes). These results indicate that although measurements are generally consistent when measured in different frequency bands, some individual measurements do change significantly. Also, there is a tendency for measurements to be smaller at higher frequencies (points lie slightly to the right of the lines in Figure 8). These results indicate that spectral magnitudes can be measured in different frequency bands, but with some caution and attention to spectral shape variations.

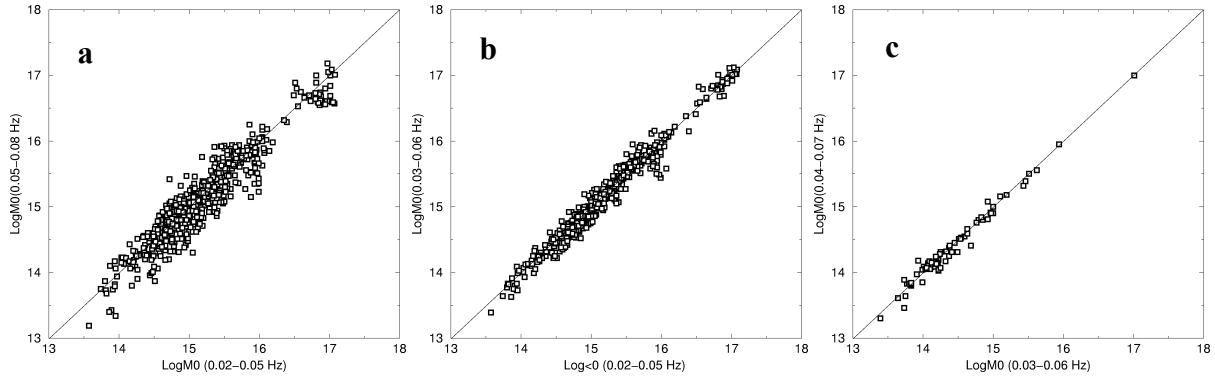


**Figure 8. Comparison of station spectral magnitudes in different frequency bands: (a) adjacent bands, all distances; (b) overlapping bands, all distances; (c) overlapping bands, distances ≤5$^o$.**

Finally, we examine which frequency bands perform best for discrimination between small earthquakes and explosions. That is, we want to find out if any set of variable frequencies would perform better in terms of discrimination than a single frequency band applied at all distances. Figure 9 shows log$M_0$:$m_b$ plots using a set of variable frequencies (0.02-0.05 Hz for distances exceeding $25^0$, 0.06-0.09 Hz for $10^0$ to 250, and 0.08-0.11 Hz for distances below $10^0$) and the 0.03-0.07 Hz frequency band for all distances. The plot on the left, where higher frequencies are used at small distances (and hence for the smallest earthquakes) apparently has a lower discriminating power for small events than when 0.03-0.07 Hz magnitudes are used. The reason is that the spectral magnitudes of smaller events (log$M_0$ 14 to 15; i.e., $M_s$ 2.2 to 3.2), recorded predominantly at regional distances, are generally smaller than the estimates at lower frequencies. We examined the log$M_0$:$m_b$ ratio for a number of frequency bands and established that the 0.03-0.07 Hz interval performs best in discriminating between earthquakes and explosions for the Lop Nor

data set. The performance of the time domain $M_s$:$m_b$ discriminant for these events (not shown), is similar to that of the variable frequency measurement (Figure 9, left), although the comparison is complicated by the fact that there is not a standard procedure for measuring time domain *Ms* in the regional distance range.

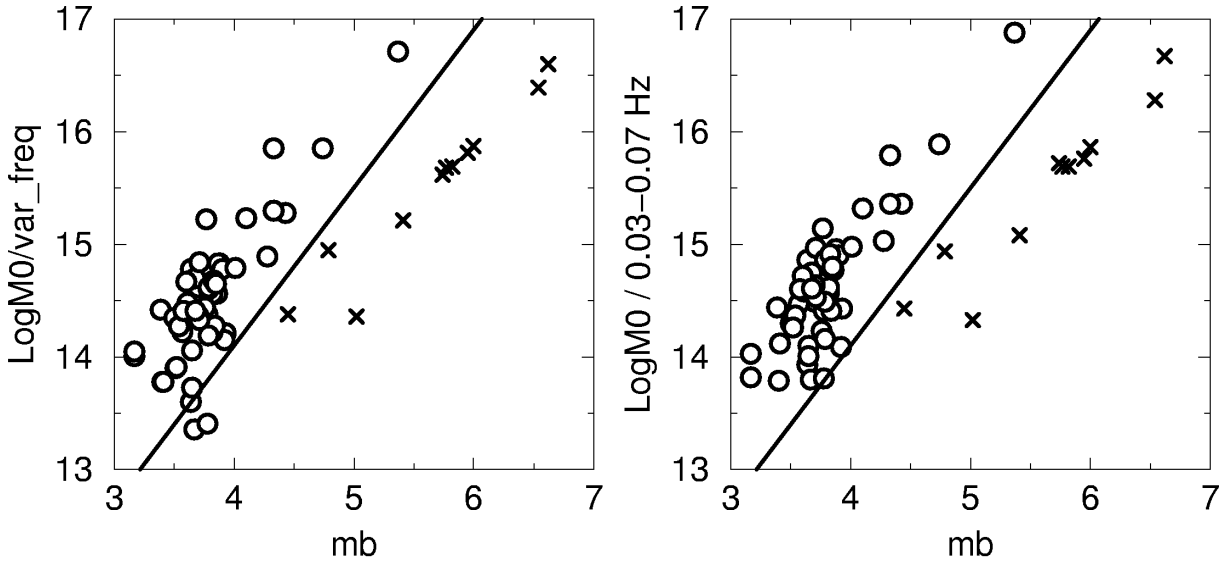


**Figure 9. Log$M_0$:$m_b$ plots showing event spectral magnitudes for earthquakes (O) and explosions (X) in Lop Nor. Station spectral magnitudes were calculated using frequencies increasing with distance (left) and the 0.03-0.07 Hz frequency band for all distances (right). Bold lines mark the empirical discrimination relationship of Stevens and McLaughlin (2001).**

## CONCLUSIONS AND RECOMMENDATIONS

Improvements to surface wave dispersion models are being accomplished by: 1) continuing addition of new data with good quality control and particular attention to regions with gaps in data coverage; 2) removal of poor quality data in the data set (poor quality data becomes more apparent as the data set increases and the model quality improves); 3) addition of model types where the data requires them; 4) improvement in constraints on sediments and Moho thickness; 5) improvement to the regularization techniques, which can now be defined on a model by model basis, allowing improved data fit while achieving realistic earth models.

Improved methods for surface wave measurement are being implemented and tested. Surface wave spectra are derived from phase-matched filtered data, and the phase-matched filters are derived from the regionalized dispersion models. Path corrected spectral magnitudes are derived by dividing the observed spectra by an explosion Green's function, where the Green's functions are calculated from the global earth models. Thus we use the earth and dispersion models to optimize spectral measurements and regionalize surface wave excitation and attenuation. In this paper, we have described a detailed study of procedures for optimizing measurement of path corrected spectral magnitudes. A significant advantage of log$M_0$ over $M_s$ is that it can be measured at any distance range without the anomalies caused by variations in dispersion that affect $M_s$. In principle, log$M_0$ can be measured over any frequency band and optimized by choosing the band with maximum S/N. However, we found that log$M_0$ for earthquakes is frequently significantly lower at higher frequencies, which degrades discrimination, and that furthermore the S/N for lower frequencies is good even for very short distances. We therefore recommend that surface wave measurements be made at lower frequencies even at short distances. We are in the process of determining the optimum frequency band for measurement, and our current recommendation is to use a frequency band of 0.03-0.07 Hz consistently for all data. We are continuing to evaluate this recommendation for a larger data set with more types of earth structure.

**ACKNOWLEDGEMENTS**

We would like to thank Mike Ritzwoller, Anatoli Levshin and Nikolai Shapiro of the University of Colorado, Bob Herrmann of St. Louis University, and other researchers who have allowed us to use their data in this project.

**REFERENCES**

Bassin, C., G. Laske, and G. Masters (2000), The Current Limits of Resolution for Surface Wave Tomography in North America, *EOS Trans AGU* 81, F897.

Ekstrom, G., A. M. Dziewonski, G. P. Smith, and W. Su (1996), Elastic and Inelastic Structure Beneath Eurasia, in *Proceedings of the 18th Annual Seismic Research Symposium on Monitoring a Comprehensive Test Ban Treaty, 4-6 September, 1996*, Phillips Laboratory Report PL-TR-96-2153, July, ADA313692, 309-318.

Engdahl, E. R., R. van der Hilst, and R. Buland (1998), Global Teleseismic Earthquake Relocation with Improved Travel Time and Procedures for Depth Determination, *Bull. Seismol. Soc. Am.* 88, 722 - 743.

Hansen, P. C. (1998), Rank-Deficient and Discrete Ill-Posed Problems, SIAM, Philadelphia, 1998.

Huang, Z., W. Su, Y. Peng, Y. Zheng, and H. Li (2003), Rayleigh Wave Tomography of China and Adjacent Regions. *J. Geophys. Res.* 108(B3), 2073, doi: 10.1029/2001JB001696.

Kennett, B. L. N. E. R. Engdahl, and R. Buland (1995), Constraints on Seismic Velocities in the Earth from Travel Times, *Geophys. J. Int.* 122**,** 108-124.

Laske, G. and G. Masters (1997), A Global Digital Map of Sediment Thickness, *EOS Trans. AGU* 78, F483.

Laske, G., G. Masters, and C. Reif, Crust 2.0 (2001): A New Global Crustal Model at 2x2 Degrees, http://mahi.ucsd.edu/Gabi/rem.html.

Levshin, A., J. L. Stevens, M. H. Ritzwoller, and D. A. Adams (2002), Short Period (7s-15s) Group Velocity Measurements and Maps in Central Asia, in *Proceedings of 24th Seismic Research Review - Nuclear Explosion Monitoring: Innovation and Integration, 17-19 September 2002*, 97-106.

Marshall, P. D. and P. W. Basham (1972), Discrimination Between Earthquakes and Underground Nuclear Explosions Employing an Improved $M_s$ Scale, *Geophys. J. R. astr. Soc.* 28, 431-458.

Mooney, W., G. Laske, and G. Masters (1998), Crust 5.1: A Global Crustal Model at 5x5 Degrees, *J. Geophys. Res.* 103, 727-747.

Stevens, J. L. and D.A. Adams (2000), Improved Surface Wave Detection and Measurement Using Phase-Matched Filtering and Improved Regionalized Models, in *Proceedings of the 23rd Seismic Research Review: Worldwide Monitoring of Nuclear Explosions, 12-15 September 2000*, 145-154.

Stevens, J. L., D.A. Adams, and G. E. Baker (2001a), Improved Surface Wave Detection and Measurement Using Phase-Matched Filtering with a Global One Degree Dispersion Model, in *Proceedings of the 23rd Annual DOD/DOE Seismic Research Symposium, 1-5 October 2001*, 420-430.

Stevens, J. L., D. A. Adams, and E. Baker (2001b), *Surface Wave Detection and Measurement Using a One Degree Global Dispersion Grid*, SAIC Final Report to Defense Threat Reduction Agency, SAIC-01/1084, December.

Stevens, J. L., D. A. Adams, and E. Baker (2002), Improved Surface Wave Dispersion Models and Azimuth Estimation Techniques, in *Proceedings of 24th Seismic Research Review - Nuclear Explosion Monitoring: Innovation and Integration, 17-19 September 2002*, 552-561.

Stevens, J. L. and K. L. McLaughlin (2001), Optimization of Surface Wave Identification and Measurement, *Pure Appl. Geophs.* 158, 1547-1582.

Yang, X., S. R. Taylor, H. J. Patton, M. Maceira, and A. A. Velasco (2002), Evaluation of Intermediate-Period (10- to 30-sec) Rayleigh-Wave Group Velocity Maps for Central Asia, in *Proceedings of 24th Seismic Research Review - Nuclear Explosion Monitoring: Innovation and Integration, 17-19 September 2002,* 609-617.